

SCIENTIFIC REPORTS

OPEN

Salinity and Conductivity Amendment of Soil Enhanced the Bioelectrochemical Degradation of Petroleum Hydrocarbons

Xiaojing Li^{1,2}, Xin Wang², Yueyong Zhang², Qian Zhao², Binbin Yu³, Yongtao Li¹ & Qixing Zhou²

Received: 22 April 2016

Accepted: 16 August 2016

Published: 06 September 2016

The extreme salinity and high internal resistance of saline-alkali soil contaminated by petroleum hydrocarbons were two key limitations for using the bioelectrochemical remediation. In order to solve two problems, we simply rinsed soil, added carbon fiber to polluted soil. The charge output was enhanced by 110% with increase of the maximum current densities from 81 to 304 mA·m⁻² while hydrocarbons degradation rate enhanced by 484%, especially the high molecular weight fractions (C28–C36 of *n*-alkanes and 4–6 rings of PAHs). These effects were possibly due to the selective enrichment of species belonged to δ -*Proteobacteria* (*Proteobacteria*), *Flavobacteriia* (*Bacteroidetes*) or *Clostridia* (*Firmicutes*), the activities of biological electron transfer and enzymes. As we know, oxygenase gene that directly decided the process of degradation, was surveyed for the first time in soil bioelectrochemical remediation system. The results confirmed that the bio-current stimulated the activities of naphthalene dioxygenase and xylene monooxygenase and thus the hydrocarbons degradation and the electricity generation. Given that electricity generation and the remediation performance are governed by multiple factors, understanding of microbial community and enzyme gene is crucial to promote the power yield and the bioelectrochemical remediation applicability.

Remediation of soils contaminated by petroleum hydrocarbons has been an arduous task, which attracts increasing attention since certain highly toxic and recalcitrant compounds are involved^{1,2}. Physical and chemical remediation inevitably destroyed the original habitat and caused secondary pollution^{3,4}. Though regular microbial technology and phytoremediation exert little effect on the pristine environment^{5,6}, they are seriously restricted by ambient conditions (especially remote/extreme environment). Bioelectrochemical remediation, as an emerging technology, applies inexhaustible electrodes as the terminal electron acceptors to enhance biodegradation with the advantage of energy recovery^{7–13}. Cost of remediation is greatly decreased as well as the scope is extended^{10,14,15}. The soil microbial fuel cell (MFC) is one of commonly electrochemical biostimulation approaches and hardly exerts adverse influence on original soil structures and properties. Low cost, high efficiency and prevalent application are driving soil MFCs to be adopted widely.

Salt-influenced soils represent around 40% of the world's lands¹⁶. Petroleum hydrocarbons contaminated saline-alkali soil is a common polluted environment because great oilfields always locate in coastal area. Due to the unfavorable high osmotic potential imposed by salts, the saline condition limits the activity of microorganism^{17,18}. Qin *et al.* found that the degradation rate of petroleum hydrocarbons increased by about 30% when the soil salinity decreased from 2.86‰ to 0.10‰¹⁸. Furthermore, high internal resistance is a key limiting factor to performance of MFCs^{19–22}, particular in soil/sediment due to the low electrical conductivity^{23,24}. It was noted that a 57% of decrement in internal resistance lead to a 100% of increment in current density in soil MFCs²⁵. Additionally, our previous study found that U-type soil MFC with 7.4 Ω of internal resistance exhibited better performance of petroleum hydrocarbons degradation and power generation, compared to that with 42.6 Ω ¹⁰.

¹Agro-Environmental Protection Institute, Ministry of Agriculture, Tianjin 300191, China. ²MOE Key Laboratory of Pollution Processes and Environmental Criteria/Tianjin Key Laboratory of Environmental Remediation and Pollution Control/College of Environmental Science and Engineering, Nankai University, Tianjin 300071, China. ³College of Environmental Science and Engineering, Yangzhou University, Yangzhou 225127, China. Correspondence and requests for materials should be addressed to X.W. (email: xinwang1@nankai.edu.cn) or Q. Zhou (email: zhouqx@nankai.edu.cn)

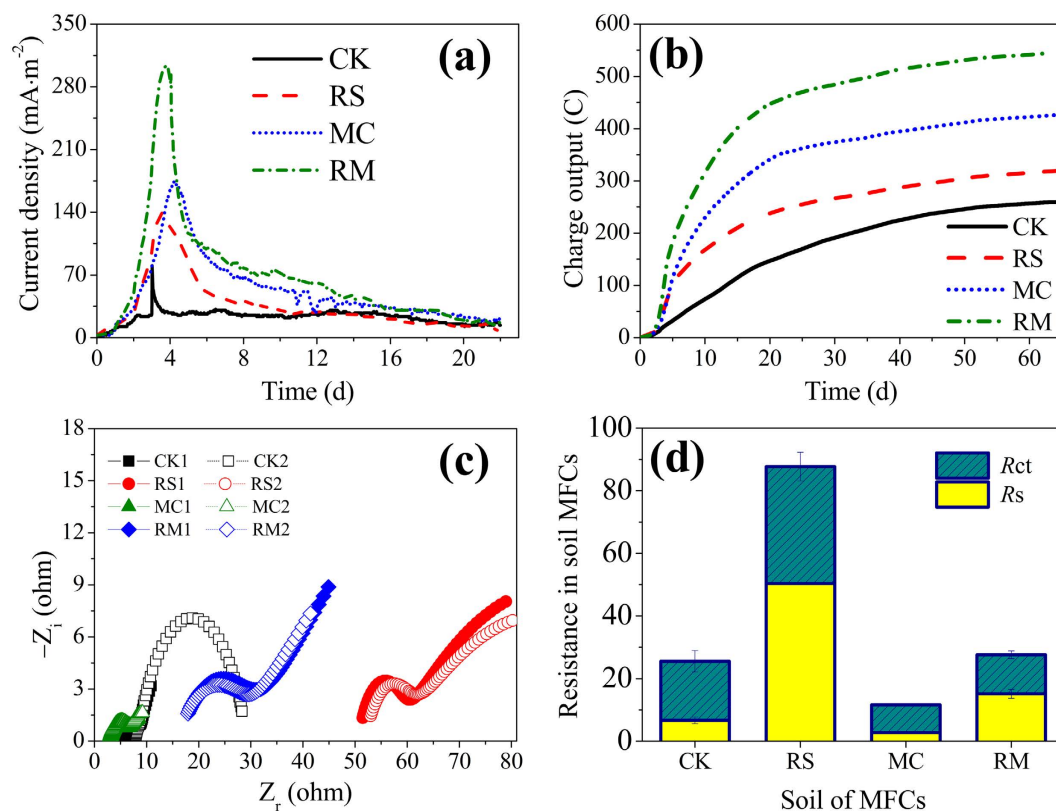


Figure 1. Current density during initial 22 days (a) and charge output during a period of 65 days (b) of the soil MFCs. The data is the mean value of duplicate soil MFCs (see Figure S1). Nyquist plots of the soil MFCs at open circuit potentials (c). The resistance analysis of the soil MFCs (d). The charge transfer resistance $R_{ct} = R_{cathode} + R_{anode}$.

Herein, two treatments including were conducted to enhance bioelectrochemical remediation of petroleum hydrocarbons contaminated saline-alkali soil. The performances of soil MFCs were investigated in terms of power generation, soil characteristics, hydrocarbons degradation, bacterial abundances. More importantly, oxygenase genes that have been widely used for the molecular monitoring of hydrocarbons biodegradation, were firstly quantified in soil MFCs. Simultaneously comprehensive correlations were surveyed to further understand the interaction among these factors in the bioelectrochemical remediation system.

Results

Performance of the soil MFC. The current densities of all treatments including RS, MC and RM were enhanced compared to CK (Fig. 1a and Figure S1a). The maximum current density of RS ($135 \pm 2 \text{ mA} \cdot \text{m}^{-2}$, averaged over 12 h of peak current) and MC ($170 \pm 2 \text{ mA} \cdot \text{m}^{-2}$, averaged over 12 h of peak current) were 214% and 295% higher than that of CK ($43 \pm 11 \text{ mA} \cdot \text{m}^{-2}$, averaged over 12 h of peak current). The peak of current density of RS was observed after 85 h, which was 16 h earlier than that of MC. Meanwhile, RS had the highest current density during initial 24 hours (Figure S2). For RM, $299 \pm 4 \text{ mA} \cdot \text{m}^{-2}$ of maximum current density was acquired on day 4 and was 595%, 121% and 76% higher than CK, RS and MC respectively. The accumulated charge output of $260 \pm 51 \text{ C}$ for CK was gained during 65 days, which was 23%, 64% and 110% lower than these of RS ($320 \pm 82 \text{ C}$), MC ($427 \pm 91 \text{ C}$), and RM ($546 \pm 43 \text{ C}$) respectively (Fig. 1b and Figure S1b).

RS had the highest internal resistance of $88 \pm 5 \Omega$, which was 238% higher than that of CK ($26 \pm 4 \Omega$), while the lowest internal resistance ($12 \pm 0 \Omega$) was observed in MC (Fig. 1c,d). There was no significant difference on total internal resistance between CK and RM ($26 \pm 2 \Omega$). For the soil samples rinsed salt (RS and RM), the Ohmic resistance (R_s) increased. Particularly, R_s of RS ($50 \pm 0 \Omega$) enlarged by more than a factor of 6 compared to CK ($7 \pm 1 \Omega$). However, R_s of MC ($3 \pm 0 \Omega$) was only 43% of CK. Charge transfer resistances (R_{ct}) exhibited a similar trend to the total internal resistances.

Changes of soil characteristic. In the connected soil MFCs, soil pH decreased compared with original soil (OS, 8.30 ± 0.04) or rinsed salt original soil (RSOS, 9.08 ± 0.02) (Figure S3a). For CK and MC, only a 3–4% drop than OS was observed. While soil pH of RS and RM described a 10–13% lower than RSOS. For the connected MFCs, soil pH exhibited a slight differentiation. The soil electrical conductivities of RS ($0.61 \pm 0.01 \text{ mS} \cdot \text{cm}^{-1}$) and RM ($1.51 \pm 0.00 \text{ mS} \cdot \text{cm}^{-1}$) were 110% and 419% higher than that ($0.29 \pm 0.00 \text{ mS} \cdot \text{cm}^{-1}$) of RSOS (Figure S3b). While CK ($0.92 \pm 0.00 \text{ mS} \cdot \text{cm}^{-1}$) and MC ($1.33 \pm 0.00 \text{ mS} \cdot \text{cm}^{-1}$) showed 49% and 27% of decline from OS ($1.81 \pm 0.04 \text{ mS} \cdot \text{cm}^{-1}$). The soil electrical conductivities of connected soil MFCs showed a 14–49% of decrease

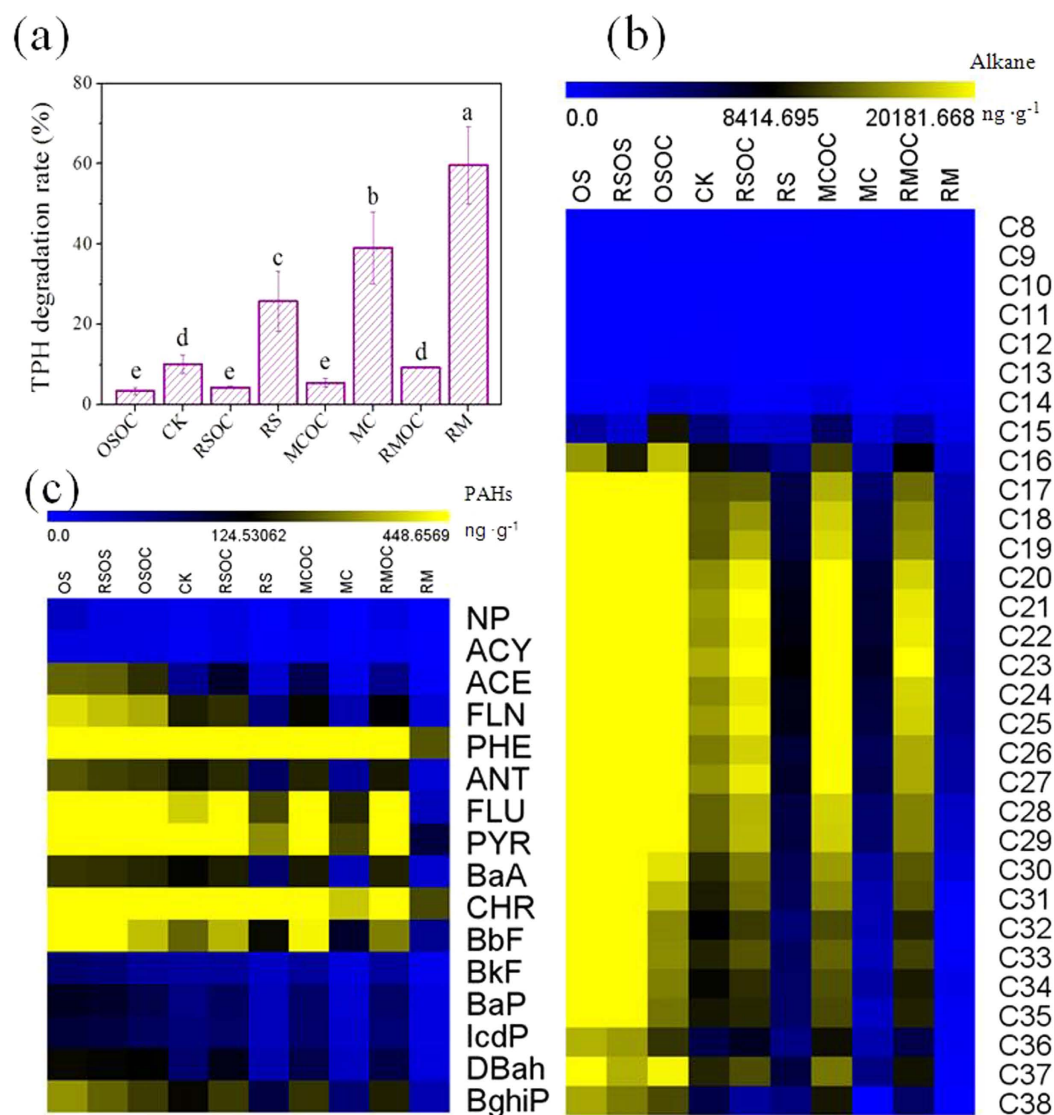


Figure 2. TPH degradation rates (a), concentrations of the *n*-alkanes (C8–C38) (b) and 16 priority PAHs (c) in soil of MFCs. The abbreviations of PAHs were noted in Figure S5. The different lowercase indicates significant difference at the 0.01 level (2-tailed).

from their corresponding controls. Both soil dehydrogenase and polyphenol oxidase activities in connected MFCs were much lower than those of OS or RSOS (Figure S3c,d). In addition, RS, MC or RM depicted lower enzyme activities than CK. Compared to the soil dehydrogenase, the soil polyphenol oxidase showed insignificant differences after bioelectrochemical remediation.

The soluble TC content of RSOS ($419 \pm 18 \mu\text{g} \cdot \text{g}^{-1}$) was only 75% of the OS ($560 \pm 30 \mu\text{g} \cdot \text{g}^{-1}$), which was partly accounted for the lower TC contents in rinsed salt soil samples (RS and RM) compared to CK and MC (Figure S4). Yet the soluble TN of RSOS ($4.4 \pm 0.3 \mu\text{g} \cdot \text{g}^{-1}$) was comparable to the OS ($4.8 \pm 0.8 \mu\text{g} \cdot \text{g}^{-1}$) indicating that nonionic nitrogen species were dominated in original soil. For all soil samples, TC and TN in connected MFCs showed 10–25% and 28–72% of reduction from the disconnected MFCs. Total organic carbon (TOC) was the main component of soluble TC in tested soil, and the dominant decrease of TC was inorganic carbon (IC) for CK and MC while TOC for RS and RM. Noticeably, the TN of soil in tested MFCs showed a evident increase (a factor of 16–70) from OS (or RSOS).

Degradation of hydrocarbons. As shown in Fig. 2a, the degradation rates of total petroleum hydrocarbons (TPHs) exhibited 153–484% of increment from CK in the connected MFCs after 65 days. Compared to their controls, the TPHs degradation rates in the connected MFCs were significantly ($p < 0.01$) higher and enhanced by a factor of 2–6. The highest degradation rate of TPHs was $60 \pm 9\%$ in RM, which was more than a factor of 20 as high as that in OSOC ($3 \pm 1\%$). The removal rates of TPHs were as follow: $\text{RM} > \text{MC} > \text{RS} > \text{CK}$.

Similar to TPHs, the contents of *n*-alkanes and PAHs were obviously reduced (Fig. 2b,c) and showed 59–92% and 44–88% of overall degradation rates in the connected MFCs (Figure S6). As expected, the concentration of

n-alkanes and PAHs in the connected MFCs were much lower than those in the disconnected MFCs. In addition to the carbon fractions of C16–C19, the high molecular weight fractions (C28–C36) also showed an obvious reduction, particular in RM (Fig. 2b and Figure S6b). Generally the higher degradation rates were observed on low ring of PAHs (1–3 rings, C10–C13) over high ring PAHs (Fig. 2c and Figure S6d). However, even the high molecular weight of PAHs (4–6 rings, C16–C22) were degraded apparently after soil MFC remediation.

Microbial community structures. According to the pyrosequencing of soil samples, the high-quality 16S rRNA gene 10492–20955 reads with an average length of 396 bp were constructed (Table S1). These sequences were assigned into 523–747 OTUs at a 97% similarity. Although new bacterial phylotypes continued to emerge even after 15,000 reads sampling with pyrosequencing, Shannon Index showed a plateau after 10,000 reads (Figure S7). This was also supported by 98–99% of Coverage estimators (Table S1), showing that the sizes of libraries were sufficient to cover the bacterial communities. The connected MFCs described the larger ACE and Chao 1 Index than those of the disconnected MFCs, while an inverse tendency was viewed for Shannon Index. Moreover, the highest ACE and Chao 1 estimators in RS indicated that its community had the greatest richness. The higher Shannon Index was observed in CK than others, showing that its biodiversity was most abundant.

Distinct cluster of bacterial communities were observed between rinsed and not rinsed salt soil samples, as well as between connected and disconnected MFCs from the hierarchical cluster analysis (Fig. 3). This was supported by principal component analysis (PCA) (Figure S8). Principal components 1 and 2 explained 40.32% and 25.62% of the total community variations, respectively. The sum of total observed OTUs in four communities of the connected MFCs was 1340, and 40% (537 OTUs) of the total OTUs were shared by them. OTUs of CK were the most (1073, 80% of total). The rest were as follow: RS (990, 74%) > MC (928, 69%) > RM (851, 64%), directly demonstrated that a selective enrichment was induced by bio-current.

Twenty-two bacterial phyla were viewed from eight libraries (Fig. 4a). The absolute majority of sequences belonged to *Proteobacteria* that accounted for 34–71% of the total reads in bacterial community. γ -*Proteobacteria* was the most abundant class (20–85%) within the *Proteobacteria*, but its ratio reduced by 49–215% in connected MFCs compared to those in disconnected MFCs except RM (Fig. 4b). α -*Proteobacteria* abundance exhibited a similar trend to γ -*Proteobacteria*. In addition, the abundance of β -*Proteobacteria* rose in CK and RS, but declined in MC and RM. In comparison, an increase of composition was observed for δ -*Proteobacteria* in all connected MFCs compared with the corresponding disconnected MFCs.

Furthermore, the *Bacteroidetes*, *Firmicutes*, *Acidobacteria* and a certain amount of unclassified sequences (at the phylum level) were other major bacterial phyla. Compared to their controls, *Bacteroidetes* and *Firmicutes* abundances in connected MFCs increased while *Acidobacteria* abundance decreased in MC and RM. Within *Bacteroidetes*, the proportion of *Flavobacteriia* was the highest (Fig. 4c). *Bacteroidia* abundance described an increment, but a decrement for *Cytophagia*. Within *Firmicutes*, *Bacilli* and *Clostridia* were the majority (97.8–99.9%) in all soil MFCs (Fig. 4d). In connected MFCs, the ratio of *Bacilli* declined, but *Clostridia* rose.

The distribution of bacterial species at genus level was presented by a heat map (Fig. 3), which accounted for 70–84% of total composition in all libraries (genera that were less than 2% of total composition were ignored, Table S2). Similar to the results from Shannon Index, CK had the higher microbial diversity than any other. There were large number species of *Pseudomonas* (2.60–34.46%), *Salinimicrobium* (4.40–15.48%), *Bacillus* (1.33–11.64%) in all samples. The proportion of *Sedimentibacter* rose for all soil MFCs, showing a formative anaerobic environment. In CK, RS, MC and RM, the abundances of *Azospira*, *Geobacter* and *Desulfuromonas* significantly increased from their controls, particularly in RM. This increase of composition was also observed for *Desulfuromonadales* (unclassified), *Desulfitobacterium*, *Alkaliphilus*, *Castellaniella*. Abundance of *Clostridium* (unclassified) increased from 0.09% in MC to 10.35% in MCOC. In RS, *Alcanivoracaceae* as well as *Weeksella*, *Zavarzinia* and *Castellaniella* abundances showed some degree of increment, while *Bacillus* and *Pseudomonas* exhibited slight decrement compared to RSOC.

Quantification of Oxygenase. Compared to the controls, the number of copies (ng^{-1} DNA) of total bacteria (16S) showed 20–214% of increase in connected MFCs (Fig. 5), due to the stimulation of bio-current. For the individual soil MFC, there was no apparent difference between investigated naphthalene dioxygenase (*nah*) and xylene monooxygenase (*tol*) gene copies (ng^{-1} DNA), and the total of both enzyme genes accounted for 0.27–0.98% of 16S. In RS and RM, copy numbers (ng^{-1} DNA) of *nah* and *tol* significantly increased from those in corresponding controls (a factor of 5–10 and 3–5 increase for *nah* and *tol* respectively). The most copy numbers (ng^{-1} DNA) of the total of *nah* and *tol* were observed in RM, which was a factor of 7 as many as that in CK.

Discussion

The current generation of all soil MFCs peaked at around 4 days and then declined until the end of experiment, which was due to the depletion of easily biodegradable hydrocarbons²⁵. Better performance (power production and hydrocarbons degradation) for RS and MC indicated that either salinity decrease or conductivity increase of soil had positive effect for MFC remediation in saline-alkali soil. After rinsed salt, the soluble salt content of soil decreased from 2.8% to 0.3% (Table S3) so that the suppress effect from salinity on the bacterial populations (especially exoelectrogen and degradation microbe) was relieved^{18,26}. This was supported by higher current density during initial 24 h and shorter time of reaching peak current for RS. Furthermore, the internal resistance of soil blended with carbon fiber significantly declined especially R_{ct} (Fig. 1d), due probably to carbon fiber provided several conductive channels and thus promoted electron transfer and current collection, which enhanced the current density and remediation efficiency²³. Simultaneously the best performance was detected when two amendments were combined (Figs 1 and 2). As an evidence, the power generation (current density or charge output) had obviously positive correlations (0.909–0.993**) with the degradation of petroleum hydrocarbons (TPH, Alkanes and PAHs) (Table 1), confirming that bioelectrochemical remediation of soil contaminated by hydrocarbons

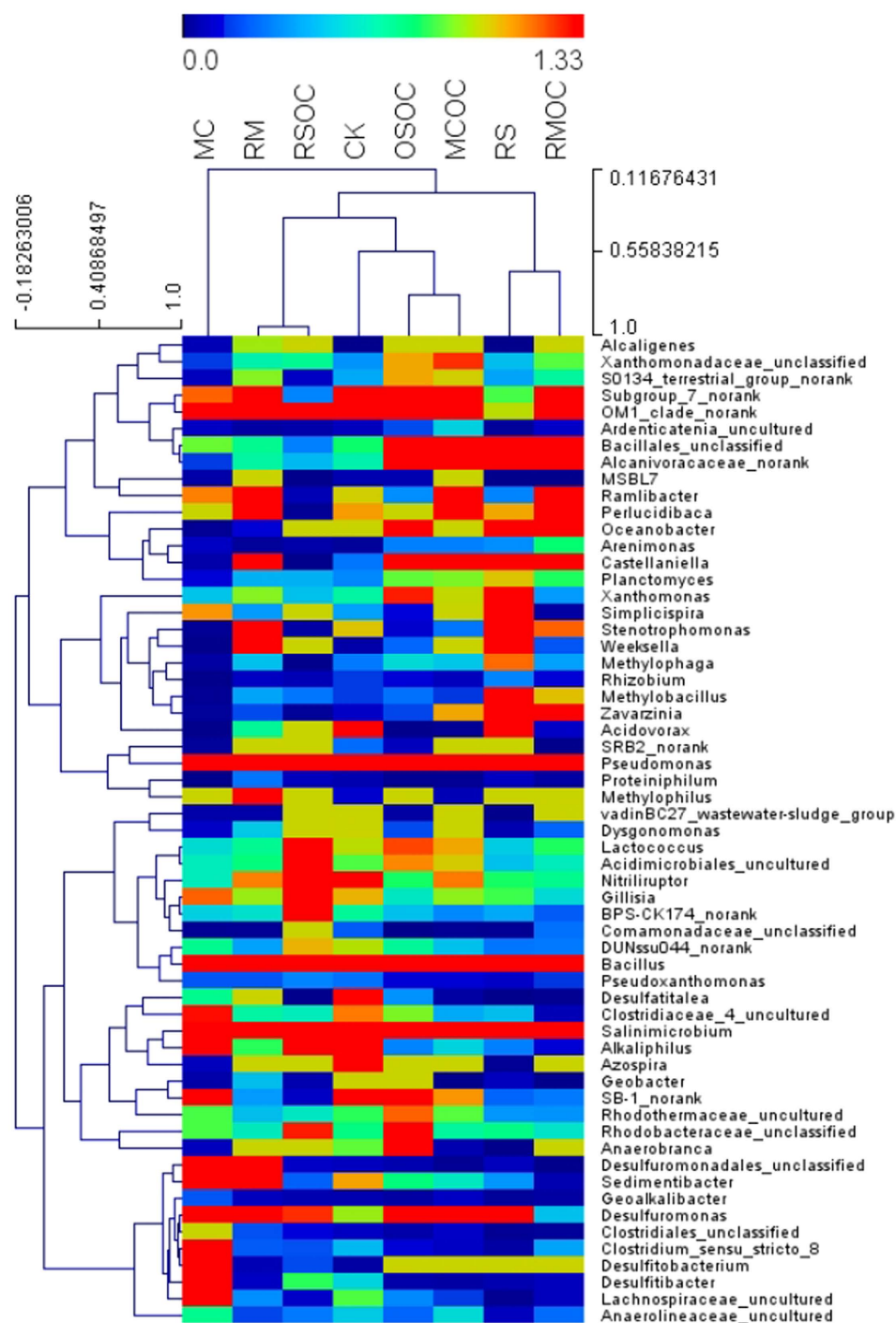


Figure 3. Taxonomic classification of bacterial DNA sequences from communities of soils in MFCs at the genus level. The genera that were less than 2% of total composition in all libraries were ignored in heat map.

was a feasible approach with the advantage of energy recovery^{7,9,12,13}. After rinsed salt, the soil osmotic pressure decreased, which was beneficial to the microbial activity. Yet the soil internal resistance significantly increased, which was adverse to the power production of soil MFC. Fortunately, the amendment treatment of blending carbon fiber completely overcame this defect. Consequently, the internal resistance of RM was comparable to that of CK (Fig. 1d). Compared to the Ohmic resistance (R_s), the charge transfer resistance (R_{ct}) had 154% and 323% more significantly negative correlations with the accumulated charge output and TPH degradation, indicating that the activity of biological electron transfer mainly determined the performance of bioelectrochemical remediation system^{20,27}.

The statistical analysis showed that the soil pH showed a lower significant correlation with the TPH degradation or the charge output than the soil electrical conductivity (Table 1), indicating that the soil electrical

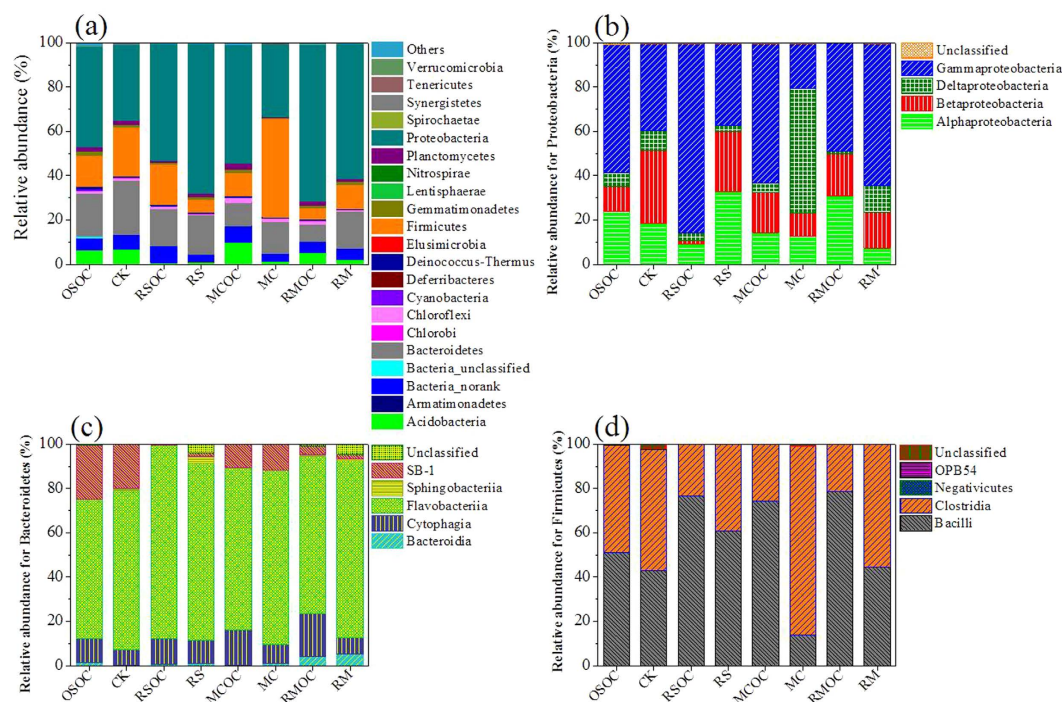


Figure 4. Taxonomic classification of bacterial DNA sequences from communities of soils in MFCs at the phylum level (a), the class level distribution of the most dominant phylum of *Proteobacteria* (b), and the following two dominant phyla, *Bacteroidetes* (c) and *Firmicutes* (d).

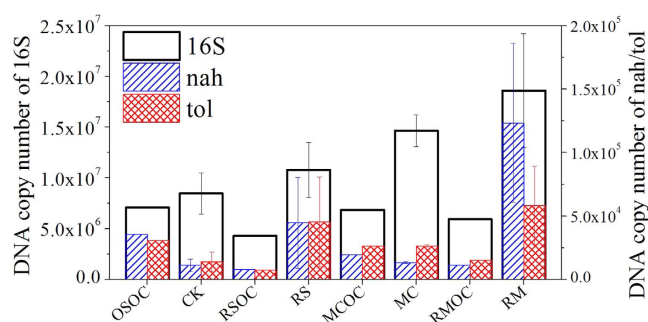


Figure 5. Real-time PCR quantification of total bacteria (16S), naphthalene dioxygenase (*nah*), xylene monooxygenase (*tol*) in different soil samples (ng⁻¹ DNA).

conductivity is a vital property in soil bioelectrochemical remediation. Additionally, the significant correlations (-0.724^* – -0.887^{**}) between enzymatic activity and petroleum hydrocarbons degradation confirmed the biodegradation stimulated by bio-current was responsible for removal of hydrocarbons. Although the soil polyphenol oxidase activity showed a less decline from the original soil (Figure S3d), a more significant correlation was viewed between soil dehydrogenase activity and TPH degradation (-0.764^*) or charge output (-0.839). Similar to previous reports⁷, these result also indicated that dehydrogenase activity may act as an bioindicator during the process of bioelectrochemical remediation.

Among abundances of top ten phyla, only *Proteobacteria*, *Firmicutes* and *Gemmatimonadetes* were positively correlated with the charge output (Table 1), indicating that a selective enrichment (e.g. exoelectrogen) was induced by bio-current^{7,13} and more importantly some species may grow by electron transfer or grow in association with specific members of the electrically active community²⁸. As an evidence, γ - and δ -*Proteobacteria* that contained the common exoelectrogens (such as *Pseudomonas* and *Geobacter*^{7,13}) showed the positive correlations with the electricity generation. Beside *Clostridia* and *Negativicutes* (Within *Firmicutes*), *Bacteroidia* abundances (within *Bacteroidetes*) were also positively correlated with the current density and charge output (0.965^* and 0.902) (Table S4). These results suggested the certain distribution of electroactive microbes. Notably, only *Proteobacteria*, *Firmicutes* and *Bacteroidetes* abundances among top ten phyla had positively correlations to hydrocarbons degradation, indicated that the main hydrocarbons degraders belonged to them^{29–31}. Significantly positive correlations between petroleum hydrocarbons degradations (TPH, alkane and PAH) and *Negativicutes*

Index	I	Q	Rs	Rct	pH	EC	DHA	PPO	TPH	Alkane	PAH
I ^a	1										
Q ^a	0.976 [*]	1									
	0.024										
Rs ^a	−0.081	−0.226	1								
	0.919	0.774									
Rct ^a	−0.433	−0.574	0.925	1							
	0.567	0.426	0.075								
pH ^b	0.338	0.23	−0.32	−0.298	1						
	0.662	0.770	0.680	0.702							
EC ^b	0.592	0.533	0.663	0.335	0.162	1					
	0.408	0.467	0.337	0.665	0.702						
DHA ^b	−0.839	−0.76	−0.461	−0.096	0.111	0.334	1				
	0.161	0.240	0.539	0.904	0.793	0.419					
PPO ^b	−0.891	−0.967 [*]	0.332	0.664	0.17	0.063	0.765 [*]	1			
	0.109	0.033	0.668	0.336	0.687	0.882	0.027				
TPH ^b	0.982 [*]	0.993 ^{**}	−0.113	−0.478	−0.004	−0.403	−0.764 [*]	−0.788 [*]	1		
	0.018	0.007	0.887	0.522	0.992	0.323	0.027	0.020			
Alkane ^b	0.909	0.945	−0.016	−0.393	−0.063	−0.514	−0.887 ^{**}	−0.724 [*]	0.930 ^{**}	1	
	0.091	0.055	0.984	0.607	0.882	0.192	0.003	0.042	0.001		
PAH ^b	0.919	0.950 [*]	−0.013	−0.391	−0.211	−0.535	−0.867 ^{**}	−0.772 [*]	0.940 ^{**}	0.966 ^{**}	1
	0.081	0.050	0.987	0.609	0.616	0.172	0.005	0.025	0.001	0.000	
Pro ^b	0.451	0.282	0.833	0.607	0.106	0.387	−0.294	−0.093	0.07	0.053	−0.013
	0.549	0.718	0.167	0.393	0.803	0.344	0.480	0.827	0.870	0.901	0.976
Bac ^b	−0.632	−0.718	−0.091	0.241	0.196	−0.578	0.172	0.432	0.04	0.062	0.101
	0.368	0.282	0.909	0.759	0.642	0.133	0.684	0.286	0.926	0.884	0.812
Fir ^b	−0.192	0.025	−0.737	−0.669	−0.196	−0.356	0.009	−0.204	0.229	0.29	0.28
	0.808	0.975	0.263	0.331	0.643	0.386	0.983	0.627	0.585	0.486	0.501
Nor ^b	−0.14	−0.206	−0.458	−0.252	0.621	0.556	0.553	0.362	−0.572	−0.671	−0.681
	0.860	0.794	0.542	0.748	0.100	0.152	0.155	0.378	0.139	0.068	0.063
Aci ^b	−0.55	−0.58	−0.419	−0.091	−0.164	0.156	0.282	0.11	−0.54	−0.58	−0.431
	0.450	0.420	0.581	0.909	0.697	0.712	0.498	0.795	0.167	0.132	0.286
Chl ^b	−0.46	−0.306	−0.845	−0.6	−0.095	0.454	0.485	0.089	−0.627	−0.671	−0.595
	0.540	0.694	0.155	0.400	0.823	0.258	0.223	0.833	0.096	0.068	0.120
Gem ^b	0.535	0.378	0.016	−0.074	0.033	0.272	0.331	0.052	−0.222	−0.487	−0.318
	0.465	0.622	0.984	0.926	0.938	0.515	0.423	0.904	0.597	0.221	0.442
Pla ^b	−0.415	−0.596	0.445	0.648	−0.168	0.352	0.245	0.209	−0.584	−0.625	−0.503
	0.585	0.404	0.555	0.352	0.690	0.392	0.558	0.619	0.129	0.098	0.204
Cya ^b	−0.115	−0.32	0.859	0.874	−0.341	0.098	0.627	0.447	−0.426	−0.626	−0.46
	0.885	0.680	0.141	0.126	0.408	0.818	0.096	0.266	0.292	0.097	0.251
Dei ^b	−0.567	−0.402	−0.747	−0.491	−0.36	−0.164	0.733 [*]	0.446	−0.416	−0.57	−0.427
	0.433	0.598	0.253	0.509	0.381	0.699	0.038	0.268	0.305	0.141	0.292

Table 1. Pearson correlation matrix (2-tailed) between dominant phyla and parameters of soil MFCs. I, the maximum current density; Q, charge output; Rs and Rct represent Ohmic and charge transfer resistance; EC, electrical conductivity; DHA, dehydrogenase; PPO, polyphenol oxidase; TPH, Alkane and PAH indicate degradation rates of total petroleum hydrocarbon, *n*-alkanes and PAHs; *Pro*, *Bac*, *Fir*, *Nor*, *Aci*, *Chl*, *Gem*, *Pla*, *Cya*, *Dei* denote *Proteobacteria*, *Bacteroidetes*, *Firmicutes*, *Bacteria_norank*, *Acidobacteria*, *Chloroflexi*, *Gemmatimonadetes*, *Planctomycetes*, *Cyanobacteria*, *Deinococcus-Thermus* respectively, which were top ten abundances at phylum level. ^an = 4. ^bn = 8. *Correlation is significant at the 0.05 level (2-tailed). **Correlation is significant at the 0.01 level (2-tailed).

abundances (0.746*–0.803*) was observed (Table S4), confirmed that *Negativicutes* play a favorable role in hydrocarbon biodegradation³². Furthermore, similar correlations were viewed between petroleum hydrocarbons degradation and *δ-Proteobacteria* (0.494–0.543), *Bacilli* (0.404–0.586). Several species of these classes found to serve an effective in the removal of petroleum hydrocarbons^{31,33}. Besides, *Planctomycetes* (−0.625), *Cyanobacteria* (−0.626), *Bacteria_norank* (−0.671), *Chloroflexi* (−0.671) closely related to *n*-alkanes degradation. These results suggested certain species (rather than all) of *Proteobacteria*, *Bacteroidetes* or *Firmicutes* played an affirmative role in degradation of hydrocarbons.

In addition to *γ-Proteobacteria* and *Bacilli*, the higher correlations between enzymatic activities and microbial abundances were observed in *Deinococcus-Thermus* and *Cyanobacteria*, nevertheless they were not the dominant

Index	I^a	Q^a	R_s^a	R_{ct}^a	pH ^b	EC ^b	DHA ^b	PPO ^b	TPH ^b	Alkane ^b	PAH ^b	16S	nah	tol
16S ^b	0.972 [*]	1.000 ^{**}	−0.219	−0.570	−0.119	−0.495	−0.725 [*]	−0.776 [*]	0.975 ^{**}	0.896 ^{**}	0.954 ^{**}	1		
	0.028	0.000	0.781	0.430	0.778	0.213	0.042	0.023	0.000	0.003	0.000			
nah ^b	0.899	0.784	0.175	−0.123	0.198	−0.173	−0.482	−0.523	0.775 [*]	0.562	0.629	0.760 [*]	1	
	0.101	0.216	0.825	0.877	0.639	0.682	0.227	0.184	0.024	0.147	0.095	0.029		
tol ^b	0.827	0.717	0.491	0.148	−0.229	−0.197	−0.573	−0.565	0.762 [*]	0.609	0.731 [*]	0.789 [*]	0.892 ^{**}	1
	0.173	0.283	0.509	0.852	0.585	0.640	0.138	0.144	0.028	0.109	0.039	0.020	0.003	

Table 2. Pearson correlation matrix (2-tailed) between gene copies and parameters of soil MFCs. 16S, total bacteria populations; nah, naphthalene dioxygenase; tol, xylene monooxygenase. ^an = 4. ^bn = 8. ^{*}Correlation is significant at the 0.05 level (2-tailed). ^{**}Correlation is significant at the 0.01 level (2-tailed).

Sample ID	Sample source
OS	Original soil
RSOS	Original soil via rinsed salt
OSOC	Disconnected MFC filled with OS
CK	Connected MFC filled with OS
RSOC	Disconnected MFC filled with RSOS
RS	Connected MFC filled with RSOS
MCOC	Disconnected MFC filled with OS mixed with carbon fiber
MC	Connected MFC filled with OS mixed with carbon fiber
RMOC	Disconnected MFC filled with RSOS mixed with carbon fiber
RM	Connected MFC filled with RSOS mixed with carbon fiber

Table 3. Abbreviations of soil samples used in this study.

hydrocarbons degraders or exoelectrogens, suggesting a subtle interaction existed between degraders and concomitant microbes. Furthermore, there were significantly positive correlations between *Deinococcus-Thermus* and *Cyanobacteria*, *Gemmatimonadetes* and *Cyanobacteria*, pointing out that a complex relationship occurred³⁴. Furthermore, the charge transfer resistance described something with the special microbial community, such as 0.957^{*} of correlation with α -*Proteobacteria*, 0.997^{*} with *Sphingobacteriia*. The change of soil characteristics directly induced the evolution of community structure³⁵. For example, increase of soil pH clearly reduced the abundance of *Acidobacteria* (Fig. 4). Additionally, soil pH had a distinctly positive correlation (0.707) with abundance of γ -*Proteobacteria* that involved in most reported exoelectrogens⁷. Moreover, there were significant correlation between soil electrical conductivity and abundance of *Bacilli* (0.715^{*}), between soil polyphenol oxidase and abundances of *Negativicutes* (−0.753^{*}), between soil dehydrogenase and *Deinococcus-Thermus* (0.733^{*}) (Table 1 and Table S4), which need to be further addressed in the succedent plan.

In bioelectrochemical remediation system, copies of naphthalene dioxygenase (nah), xylene monooxygenase (tol) exhibited a high correlation (0.899 and 0.827) with current density of soil MFCs (Table 2). Compared to nah, copies of tol had a more distinct correlation with hydrocarbon degradation (alkane and PAH). By contrast, copies of total bacteria populations (16S) obviously positively related to hydrocarbon degradation (0.896^{**}–0.975^{**}) and electricity generation (0.972^{**}–1.000^{**}), implying that biodegradable hydrocarbons was the strong determinant of total bacterial abundance and power output²⁶. Previous reports showed that amount of nah and tol could use as bioindicator in degradation of petroleum hydrocarbons contaminated soil³⁶. In soil MFCs, it was also demonstrated that the quantitative determination of key enzyme gene was feasible as a monitoring or predicting index during pollution remediation.

Methods

Tested soil and treatment. Petroleum hydrocarbon contaminated soil was collected from the topsoil (<10 cm) near the oil well in Dagang Oilfield of Binhai New Area (Tianjin, China). The soil was air-dried, passed 2 mm sieve and marked as original soil (OS). The soil properties were summarized as Table S3. The OS was rinsed with 1:1.2 (w/v) of distilled water by water leaching method¹⁸ and marked as RSOS. The connected MFCs filled with OS and RSOS were marked as CK and RS, while the corresponding disconnected controls as OSOC and RSOC. The connected MFC filled with the mixture of OS and carbon fiber pieces (1 cm of length, 5 μ m of diameter, Jilin Carbon Factory; acetone clean overnight; 2% in mass ratio to soil) was marked as MC and the corresponding disconnected control as MCOC. The MFC filled with soil that was rinsed salt and followed by blended of carbon fiber (2%), was marked as RM and its disconnected control as RMOC. The abbreviations used in this study were shown in Table 3. All soil MFCs were filled with 100 g of dry soil without adding buffer solution or any exogenous inoculation.

Soil MFC configuration. Soil MFCs were constructed as previous describe¹³ with only one layer of anode as showed in Figure S9. Carbon mesh (Jilin Carbon Factory, Jilin, China) was used as the anode after acetone clean

overnight³⁷. Activated carbon air-cathode was prepared according to the modified rolling-press method^{19,20}. All soil MFCs were placed in an incubator (30 °C) and sealed with distilled water during the experiment. Each treatment including their disconnected control had a duplicate.

Electrochemical analysis. Voltage (U) across the external resistor of 100 Ω (R) was recorded by a data acquisition system (PISO-813, ICP DAS Co., Ltd, Shanghai, China). A potentiostat (Autolab PGSTAT 302N, Metrohm, Switzerland) was used to perform electrochemical impedance spectrum (EIS) from 100 kHz to 1 Hz with a 10 mV of amplitude at the open circuit potential (stabilized for 4 h after installed). The carbon mesh anode was used as the working electrode while the air-cathode as the counter and reference electrode. ZsimpWin 3.10 was employed to simulate Nyquist plots according to an equivalent circuit in Figure S10.

Chemical analysis. The soil pH and the electrical conductivity were measured in a mixture with soil to distilled water ratio (w/v) as 1:5. Organic matter, available N, P and K were evaluated according to regular methods³⁸. The soluble salt content was measured as previous description¹⁸. The contents of metal elements were attained using ICP-OES (Vista MPX Varian, US)³⁹. The soil dehydrogenase was extracted by 2,3,5-Triphenyl Tetrazolium Chloride reduction and Triphenyl Formazone calibration (485 nm). Soil polyphenol oxidase was analyzed by catalyzing pyrogallol (430 nm) as previous methods⁴⁰. The soluble total carbon (TC) and total nitrogen (TN) were determined by an Analytik jena multi N/C 3100 (Germany) (Details found in the supporting information). The total petroleum hydrocarbon (TPH) and carbon fractions (n -alkanes and PAHs) were analyzed according to our previous procedures^{6,10}.

Biological analysis. Genomic DNA was extracted using a Power Soil DNA Isolation Kit (Mobio, USA) according to the manufacturer's instruction. 1% agarose gel electrophoresis was employed to confirm the purity of genomic DNA.

Bacterial 16S rRNA gene fragments were PCR-amplified using primers of 515F (5'-GTGCCAGCMGCCGCGG-3') and 907R (5'-CCGTCAATTCMTTTRAGTTT-3') covering V4 and V5 regions. PCR was carried out in triplicate 20 μ L reactions containing 4 μ L of 5 \times FastPfu Buffer, 2 μ L of 2.5 mM dNTPs, 0.8 μ L of each Primer (5 μ M), 0.4 μ L of FastPfu Polymerase, 10 ng of Template DNA, and added ddH₂O to bring up the final volume to 20 μ L. The PCR temperature procedures were 95 °C for 3 min; 25 cycles consisted of 95 °C for 30 s, 55 °C for 30 s and 72 °C for 45 s; 72 °C for 10 min and 4 °C until halted. After confirmed by 2% agarose gel electrophoresis, PCR products were pooled and purified using AxyPrepDNA (Axygen, USA).

Pyrosequencing was performed on a Genome Sequencer instrument (MiSeq) as the standard procedure of Majorbio Bio-Pharm Biotechnology Co., Ltd. (Shanghai, China). Quality filters were used to remove low quality sequences which were shorter than 50 bp, involved in any ambiguous bases, showed a homopolymer of longer than 10 bp, or were chimera. Finally, the valid sequences were trimmed to an average length of 396 bp. Then these sequences were clustered into Operational Taxonomic Units (OTUs) based on a 97% similarity threshold. Ribosomal Database Project classifier was used to align for their taxonomy at different levels (<http://www.arb-silva.de>).

The quantitative determination of naphthalene dioxygenase (*nah*), xylene monooxygenase (*tol*) and total bacteria populations (16S) were determined by ABI7500 FAST system with the primers⁴¹ listed in Table S5. A 25 μ L real-time PCR mixture contained 12.5 μ L of 2 \times SybrGreen qPCR Master Mix, 0.5 μ L of each primer (10 μ M), 1 μ L of Template DNA and 10.5 μ L of ddH₂O. PCR conditions were as follow: initial denaturation at 95 °C for 2 min; 40 cycles consisted of 95 °C for 10 s and 60 °C for 40 s.

Calculation. The current density ($\text{mA}\cdot\text{m}^{-2}$) of MFC was obtained as $I' = U/(R\cdot A)$, where A is the area of air-cathode (0.0036 m^2). The charge output was evaluated as $Q = \int_0^T (U/R)dt$. The degradation rate of hydrocarbons was gained as $\eta = (C_{OS} - C)/C_{OS}$, where C_{OS} is the hydrocarbons concentration in original soil (OS) or rinsed salt original soil (RSOS) as shown in Figure S10 and C is the hydrocarbons concentration in tested soil. The overall degradation rate of PAHs (or n -alkanes) was calculated by adding the contents of 16 PAHs (or 31 kinds of n -alkanes). The community richness and diversity estimates (Rarefaction, Chao 1, ACE and Shannon Index) were calculated according to the assigned methods (<http://www.mothur.org/wiki/>). Relative abundance was defined as that the number of sequences affiliated with that phylum, genus, or class divided by the total sequence number of per sample or dominant phyla (*Proteobacteria*, *Bacteroidetes* or *Firmicutes*).

References

1. Ayotamuno, M., Kogbara, R., Ogaji, S. & Probert, S. Bioremediation of a crude-oil polluted agricultural-soil at Port Harcourt, Nigeria. *Applied Energy* **83**, 1249–1257 (2006).
2. Chen, M. *et al.* Bioremediation of soils contaminated with polycyclic aromatic hydrocarbons, petroleum, pesticides, chlorophenols and heavy metals by composting: applications, microbes and future research needs. *Biotechnology Advances* **33**, 745–755 (2015).
3. Riser-Roberts, E. *Remediation of petroleum contaminated soils: biological, physical, and chemical processes*. (CRC Press, 1998).
4. Zhou, Q., Sun, F. & Liu, R. Joint chemical flushing of soils contaminated with petroleum hydrocarbons. *Environment International* **31**, 835–839 (2005).
5. Tang, J., Wang, R., Niu, X. & Zhou, Q. Enhancement of soil petroleum remediation by using a combination of ryegrass (*Lolium perenne*) and different microorganisms. *Soil and Tillage Research* **110**, 87–93 (2010).
6. Peng, S., Zhou, Q., Cai, Z. & Zhang, Z. Phytoremediation of petroleum contaminated soils by *Mirabilis jalapa* L. in a greenhouse plot experiment. *Journal of hazardous materials* **168**, 1490–1496, doi: 10.1016/j.jhazmat.2009.03.036 (2009).
7. Lu, L., Huggins, T., Jin, S., Zuo, Y. & Ren, Z. J. Microbial metabolism and community structure in response to bioelectrochemically enhanced remediation of petroleum hydrocarbon-contaminated Soil. *Environmental Science & Technology* **48**, 4021–4029 (2014).
8. Mohan, S. V. & Chandrasekhar, K. Self-induced bio-potential and graphite electron accepting conditions enhances petroleum sludge degradation in bio-electrochemical system with simultaneous power generation. *Bioresource Technology* **102**, 9532–9541 (2011).
9. Morris, J. M. & Jin, S. Enhanced biodegradation of hydrocarbon-contaminated sediments using microbial fuel cells. *Journal of hazardous materials* **213**, 474–477 (2012).

10. Wang, X., Cai, Z., Zhou, Q., Zhang, Z. & Chen, C. Bioelectrochemical stimulation of petroleum hydrocarbon degradation in saline soil using U-tube microbial fuel cells. *Biotechnology and Bioengineering* **109**, 426–433 (2012).
11. Zhang, T., Gannon, S. M., Nevin, K. P., Franks, A. E. & Lovley, D. R. Stimulating the anaerobic degradation of aromatic hydrocarbons in contaminated sediments by providing an electrode as the electron acceptor. *Environmental Microbiology* **12**, 1011–1020 (2010).
12. Zhang, Y. *et al.* Horizontal arrangement of anodes of microbial fuel cells enhances remediation of petroleum hydrocarbon-contaminated soil. *Environmental Science and Pollution Research*, 1–7 (2014).
13. Li, X. *et al.* Extended petroleum hydrocarbon bioremediation in saline soil using Pt-free multianodes microbial fuel cells. *RSC Advances* **4**, 59803–59808 (2014).
14. Yuan, Y., Chen, Q., Zhou, S., Zhuang, L. & Hu, P. Improved electricity production from sewage sludge under alkaline conditions in an insert-type air-cathode microbial fuel cell. *Journal of Chemical Technology and Biotechnology* **87**, 80–86 (2012).
15. Yuan, Y., Zhou, S. & Zhuang, L. A new approach to *in situ* sediment remediation based on air-cathode microbial fuel cells. *Journal of Soils and Sediments* **10**, 1427–1433 (2010).
16. Serrano, R. & Gaxiola, R. Microbial models and salt stress tolerance in plants. *Critical Reviews in Plant Sciences* **13**, 121–138 (1994).
17. Dendooven, L. *et al.* Dynamics of carbon and nitrogen in an extreme alkaline saline soil: a review. *Soil Biology and Biochemistry* **42**, 865–877 (2010).
18. Qin, X., Li, D., Tang, J., Zhang, Q. & Gao, J. Effect of the salt content in soil on bioremediation of soil by contaminated petroleum. *Letter in Applied Microbiology* **55**, 210–217 (2012).
19. Li, X., Wang, X., Zhang, Y., Ding, N. & Zhou, Q. Opening size optimization of metal matrix in rolling-pressed activated carbon air-cathode for microbial fuel cells. *Applied Energy* **123**, 13–18 (2014).
20. Li, N., Liu, Y., An, J., Feng, C. & Wang, X. Bifunctional quaternary ammonium compounds to inhibit biofilm growth and enhance performance for activated carbon air-cathode in microbial fuel cells. *Journal of Power Sources* **272**, 895–899, doi: 10.1016/j.jpowsour.2014.09.008 (2014).
21. Cheng, S., Liu, H. & Logan, B. E. Increased power generation in a continuous flow MFC with advective flow through the porous anode and reduced electrode spacing. *Environmental Science & Technology* **40**, 2426–2432 (2006).
22. Liu, H., Cheng, S. & Logan, B. E. Power generation in fed-batch microbial fuel cells as a function of ionic strength, temperature, and reactor configuration. *Environmental Science & Technology* **39**, 5488–5493 (2005).
23. Domínguez-Garay, A., Berná, A., Ortiz-Bernad, I. & Esteve-Núñez, A. Silica colloid formation enhances performance of sediment microbial fuel cells in a low conductivity soil. *Environmental Science & Technology* **47**, 2117–2122 (2013).
24. Rezaei, F., Richard, T. L., Brennan, R. A. & Logan, B. E. Substrate-enhanced microbial fuel cells for improved remote power generation from sediment-based systems. *Environmental Science & Technology* **41**, 4053–4058 (2007).
25. Lu, L. *et al.* Enhanced bioremediation of hydrocarbon-contaminated soil using pilot-scale bioelectrochemical systems. *Journal of hazardous materials* **274**, 8–15 (2014).
26. Nie, M. *et al.* Rhizosphere effects on soil bacterial abundance and diversity in the Yellow River Deltaic ecosystem as influenced by petroleum contamination and soil salinization. *Soil Biology and Biochemistry* **41**, 2535–2542 (2009).
27. Wetser, K., Sudirjo, E., Buisman, C. J. & Strik, D. P. Electricity generation by a plant microbial fuel cell with an integrated oxygen reducing biocathode. *Applied Energy* **137**, 151–157 (2015).
28. Wrighton, K. C. *et al.* A novel ecological role of the Firmicutes identified in thermophilic microbial fuel cells. *The ISME journal* **2**, 1146–1156 (2008).
29. Kostka, J. E. *et al.* Hydrocarbon-degrading bacteria and the bacterial community response in Gulf of Mexico beach sands impacted by the Deepwater Horizon oil spill. *Applied and environmental microbiology* **77**, 7962–7974 (2011).
30. Röling, W. F. *et al.* Robust hydrocarbon degradation and dynamics of bacterial communities during nutrient-enhanced oil spill bioremediation. *Applied and environmental microbiology* **68**, 5537–5548 (2002).
31. Al-Mailem, D., Kansour, M. & Radwan, S. Bacterial communities associated with biofouling materials used in bench-scale hydrocarbon bioremediation. *Environmental Science and Pollution Research* **22**, 3570–3585 (2015).
32. de Menezes, A., Clipson, N. & Doyle, E. Comparative metatranscriptomics reveals widespread community responses during phenanthrene degradation in soil. *Environmental microbiology* **14**, 2577–2588 (2012).
33. Trejo-Hernandez, M., Ortiz, A., Okoh, A., Morales, D. & Quintero, R. Biodegradation of heavy crude oil Maya using spent compost and sugar cane bagasse wastes. *Chemosphere* **68**, 848–855 (2007).
34. Logan, B. E. Exoelectrogenic bacteria that power microbial fuel cells. *Nature Reviews Microbiology* **7**, 375–381 (2009).
35. Lauber, C. L., Strickland, M. S., Bradford, M. A. & Fierer, N. The influence of soil properties on the structure of bacterial and fungal communities across land-use types. *Soil Biology and Biochemistry* **40**, 2407–2415 (2008).
36. DeBruyn, J. M., Chewing, C. S. & Saylor, G. S. Comparative quantitative prevalence of Mycobacteria and functionally abundant *nidA*, *nahAc*, and *nagAc* dioxygenase genes in coal tar contaminated sediments. *Environmental Science & Technology* **41**, 5426–5432 (2007).
37. Wang, X. *et al.* Use of carbon mesh anodes and the effect of different pretreatment methods on power production in microbial fuel cells. *Environmental Science & Technology* **43**, 6870–6874 (2009).
38. Liu, G. *Soil physical and chemical analysis and description of soil profiles*. (China Standard Press, 1996).
39. Sun, Y., Zhou, Q., Xie, X. & Liu, R. Spatial, sources and risk assessment of heavy metal contamination of urban soils in typical regions of Shenyang, China. *Journal of hazardous materials* **174**, 455–462 (2010).
40. Zhou, L. *Soil enzymology*. (Science and Technology Press, 1987).
41. Baldwin, B. R., Nakatsu, C. H. & Nies, L. Detection and enumeration of aromatic oxygenase genes by multiplex and real-time PCR. *Applied and Environmental Microbiology* **69**, 3350–3358 (2003).

Acknowledgements

This research work was financially supported by the Natural Science Foundation of Tianjin (No. 16JCQNJC08800), the Ministry of Science and Technology as an 863 major project (No. 2013AA06A205), the National Natural Science Foundation of China (No. 41601536, 21577068 and 51409052), and the Special Fund for Agro-Scientific Research in the Public Interest of China (No. 201503107-7).

Author Contributions

X.L. and X.W. designed the research; X.L., Y.Z., Q.Z., B.Y. and Y.L. performed the research; X.L. and Q.Z. analyzed the data and wrote the paper; and X.W. and Q.Z. revised the manuscript.

Additional Information

Supplementary information accompanies this paper at <http://www.nature.com/srep>

Competing financial interests: The authors declare no competing financial interests.

How to cite this article: Li, X. *et al.* Salinity and Conductivity Amendment of Soil Enhanced the Bioelectrochemical Degradation of Petroleum Hydrocarbons. *Sci. Rep.* **6**, 32861; doi: 10.1038/srep32861 (2016).



This work is licensed under a Creative Commons Attribution 4.0 International License. The images or other third party material in this article are included in the article's Creative Commons license, unless indicated otherwise in the credit line; if the material is not included under the Creative Commons license, users will need to obtain permission from the license holder to reproduce the material. To view a copy of this license, visit <http://creativecommons.org/licenses/by/4.0/>

© The Author(s) 2016